NIST Special Publication 260-195

Certification of Standard Reference Material® SRM 2687a

Portland Cement Clinker

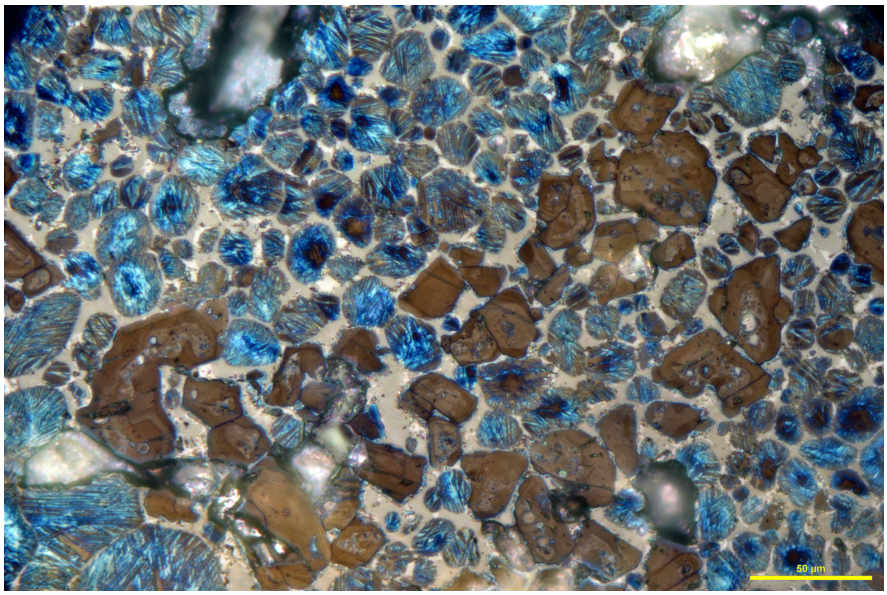

Paul Stutzman
Alan Heckert

This publication is available free of charge from:
https://doi.org/10.6028/NIST.SP.260-195

National Institute of Standards and Technology
U.S. Department of Commerce

NIST Special Publication 260-195

Certification of Standard Reference Material® SRM 2687a

Portland Cement Clinker

Paul Stutzman
Materials and Construction Division
Engineering Laboratory

Alan Heckert
Statistical Engineering Division
Information Technology Laboratory

This publication is available free of charge from:
https://doi.org/10.6028/NIST.SP.260-195

March 2019

U.S. Department of Commerce
Wilbur L. Ross, Jr., Secretary

National Institute of Standards and Technology
Walter Copan, NIST Director and Undersecretary of Commerce for Standards and Technology

National Institute of Standards and Technology Special Publication 260-195
Natl. Inst. Stand. Technol. Spec. Publ. 260-195, 24 pages (March 2019)
CODEN: NSPUE2

This publication is available free of charge from:
https://doi.org/10.6028/NIST.SP.260-195

Abstract

A new Standard Reference Materialtextsuperscript® (SRM) for portland cement clinker has been produced for the Office of Standard Reference Materials at the National Institute of Standards and Technology (NIST). The SRM clinkers are intended for use in developing and testing quantitative methods of phase analysis for portland cement and cement clinker. The new SRM is one of three clinkers available from NIST representing the range of textures and compositions of North American clinker production. As the original SRM stock for SRM 2687 has been depleted, new material was obtained that retained the fine-grained texture of that SRM. Certification of the phase composition of the clinker is based upon consensus means and uncertainties of two independent analytical methods: scanning electron microscopy with image analysis and x-ray powder diffraction (XRD) analyses. The XRD data were subdivided to provide two separate sample sets processed separately using two different Rietveld refinement codes. These codes differed slightly in the determination of the silicate phases, which have very similar powder diffraction patterns and can be difficult to decompose. Therefore, the input data set for determining the consensus means, uncertainties and informational values is composed of two distinct XRD phase abundance estimates and one SEM/image analysis set of estimates. The XRD data are close to that determined by microscopy, but some distinct differences are seen. The disagreements may reflect the difficulty in resolving the fine-sized aluminate and ferrite interstitial phases using the microscope and challenges in decomposing highly overlapped powder diffraction data. The XRD data do display greater precision than replicate measurements by microscopy, likely the result of the specimen homogenization resulting from grinding the clinker to a powder. The certified reference values are consensus values, calculated by combining the results from both measurement techniques using the DerSimonian-Laird method with the standard uncertainties based upon the Horn-Horn-Duncan variance estimate. Reference values are best estimates based upon a single measurement technique. Reference values are provided for phases periclase, arcanite, aphthitalite, and lime and for the bulk oxides from x-ray fluorescence analysis.

Key words

Cement clinker, consensus means, image analysis, microscopy, quantitative analysis, Rietveld analysis, x-ray powder diffraction

Table of Contents

List of Tables

List of Figures

1. Introduction

Portland cement clinker is produced by heating a mixture of limestone, shale, and iron in a cement kiln to temperatures approaching 1500 °C. The resulting sintered clinker product is subsequently ground to a fine powder with additions of gypsum and limestone to produce portland cement. Clinker comprises a set of crystalline phases that react with water to form the hydration products that bind the aggregates in portland cement concrete. Knowledge of the types and amounts of crystalline components of clinker is critical in monitoring quality control in clinker production to produce cements conforming to specific American Society for Testing and Materials (ASTM) Types, and in predicting cement performance.

The traditional approach for estimating potential phase abundance uses the indirect Bogue calculations provided in the ASTM C150 [1] specification for portland cements. This approach can be biased [2] so alternative methods used by industry include microscopy for clinker [3] and x-ray powder diffraction for clinker and cement [3]. These direct methods for analyzing clinker and cement composition have become more commonly applied since the initial offering of the SRM clinkers, providing more accurate and more complete analyses, which can lead to improved cement production and performance property prediction.

The Standard Reference Material® (SRM) clinkers are used by industry and academia for developing and testing methods of quantitative phase analysis. These clinkers were selected as representative of the range of North American clinker production with respect to phase abundance, crystal size, and crystal distribution. SRM 2687a is the latest of the three NIST reference clinkers and, with its textural characteristics similar to the original SRM 2687, is intended to replace stock of the original SRM that has now been exhausted.

The reference values represent consensus means and uncertainties based upon two independent analytical methods, quantitative XRD and image analysis of scanning electron microscope image sets. Clinker 2687a exhibits a fine-textured crystal size relative to the other clinkers, a heterogeneous phase distribution with localized nests of free lime and belite. Alite occurs as subhedral to anhedral crystals approximately 30 µm in size. Belite occurs in large clusters with an approximate crystal size of 20 µm. Periclase crystals occur occasionally throughout the microstructure at a few micrometers in size and the alkali sulfate phases arcanite and, to a lesser extent, aphthitolite are disseminated throughout the microstructure. A fine-grained ferrite is present along with a very finely intermixed (micrometer-sized) ferrite and aluminate matrix.

2. Material Selection, Sampling, and Processing

2.1 Clinker Selection

Initial screening involved obtaining a 2 kg grab sample of clinker from the plant that produced the original SRM clinker, preparing epoxy-embedded polished sections for light and electron microscopy, and grinding a subsample for x-ray powder diffraction. Because product consistency is a principal objective in cement production and because the raw ma-

terials were similar, it was anticipated that textural aspects of the clinker and phase types and amounts would remain consistent with the original SRM material. One difference in production was a change from a wet-process kiln to a dry-process. However, this change did not appear to have significantly affected the clinker texture. Microscopy confirmed the similarity to the original SRM 2687 with fine-grained clinker silicates with belite occurring in clusters and occasional streaks. A fine-grained matrix consists of aluminate and ferrite as both individual crystals and finely-intermixed and difficult to differentiate using light microscopy, but distinguished in SEM imaging. Occasional large nests of free lime occur and alkali sulfates are unevenly distributed in voids and fractures. Illustrations of these features are presented in subsequent images.

2.2 Clinker Sampling

After initial screening, about 260 kg of clinker was obtained from the plant as sieved material in a size interval ranging from 4 mm to 15 mm to sample nodules of similar thermal history. This sample was not intended to be representative of the bulk clinker production, but was sampled and processed with the intent of creating a homogeneous lot of clinker with respect to phase composition and texture. The cement kiln at the plant utilizes the dry-process and is approximately 4 m in diameter and 55 m long with a four-stage preheater and downdraft calciner. Fuel for the kiln consists of coal (75 % passing 200 mesh) and natural gas with 60 % of the fuel fired in the calciner and 40 % fired in the kiln. The kiln feed is composed of 60 % marl, 30 % high-grade limestone and 10 % combined of bauxite, iron slag and sand with a fineness of approximately 75 % passing a 200-mesh sieve. The clinker was captured by plant staff, process as detailed above and packed into sealed cartons for shipment to NIST.

2.3 Clinker Processing and Packaging

The clinker was distributed across a large sieve tray and examined to remove any loose foreign materials. A jaw crusher was used to stage-crush the clinker, a process where the crushed material is sieved, capturing the size fraction between 3 mm and 4 mm, which was set aside while the -3 mm material is discarded. The over-sized materials were re-crushed and re-sieved, once again discarding the fines that passed the 4 mm sieve until no material remained on the 4 mm sieve. The process was repeated until the entire lot of clinker had been processed. The recovery rate of the desired 3 mm to 4 mm size fraction was approximately 25 %. This material was stored in air-tight plastic bags in a sealed plastic drums and transferred to the Standard Reference Materials staff for homogenization and packaging into approximately 8400 containers. Four vials, each with about 7 g of clinker, is the base unit size.

A subset of the 8400 vials of clinker was provided by the Standard Reference Materials Program for microscopy and x-ray powder diffraction for phase characterization. Samples intended for microscopy were embedded in a low-viscosity resin under vacuum to remove accessible air from the clinker fragments. Samples for x-ray powder diffraction

Fig. 1. As-received clinker sample ready for crushing and sieving

were crushed and ground to an approximate $-10\,\mu$m median particle size. Both preparation methods are typical for the analytical method and are more completely discussed in [4].

3. Data Collection and Analysis

The traditional analytical method for examining portland cement clinker is by reflected light microscopy where the clinker is embedded in a resin, cut and polished to allow viewing of cross sections, revealing the phases and phase distribution. The clinker phases are identified by their position within the microstructure, as a framework grain, matrix, or disseminated crystal. Etchants such as water, nital, and potassium hydroxide solutions facilitate the viewing and identification of clinker phases through precipitation of reaction products which impart a coloration to the phases [5].

Use of both XRD and SEM/IA provides a complementary set of direct determinations of phase abundance. Each method has advantages in that XRD data tends to have higher precision due to the grinding of the sample while SEM data can identify constituents in low abundance. Two types of data are reported based upon the sources: 1) certified reference values that reflect a consensus between the XRD and SEM results and 2) reference values that represent a single source of data.

3.1 Light Microscopy

The light microscope is commonly used to assess production conditions by qualitatively and quantitatively evaluating clinker texture and phase abundance [5],[6],[3]. This clinker has a fine-grained matrix consisting of aluminate and ferrite, as both individual crystals and finely-intermixed. Sporadic nests of free lime occur throughout the clinker, and alkali sulfates occur intermittently as void and fracture linings. Reflected light micrographs are provided in Figure 2 for a polished cross section that has been etched with nital following a 30 s 0.1 mol L^{-1} KOH solution. The nital reacts with the silicates while the KOH reacts with the aluminates and free lime.

As discussed, clinker 2687a exhibits a fine-textured crystal size relative to the other SRM clinkers, a heterogeneous phase distribution with localized nests of free lime and belite. Alite occurs as subhedral to anhedral crystals approximately 40 µm in size and tan in color. Belite occurs as individual blue crystals as well as in large blue clusters, exhibiting the internal lameller structure, with approximate individual crystal sizes ranging between 15 µm and 50 µm. Fine-grained ferrite is present along with a very finely intermixed (micrometer-sized) ferrite and aluminate matrix. Periclase crystals occur occasionally throughout the microstructure at a few micrometers in size, and the alkali sulfate phases of arcanite and, to a lesser extent, aphthitalite are disseminated unevenly throughout the microstructure on pore and fracture perimeter coatings. Pores are seen as relatively large, irregularly-shaped voids, which may be filled with epoxy if the pore was accessible from the nodule surface, but empty and appearing with a bluish tint for open pores not accessible to the resin. SEM imaging with image analysis (IA) was also used for the microscopy analyses because the gray-scale images and complementary X-ray images are amenible for image processing and analysis to establish the quantitative phase estimates.

3.2 X-Ray Powder Diffraction

Phase composition was assessed using quantitative x-ray powder diffraction analysis following ASTM C1365 with typical powder diffraction patterns and phase identification shown in Figure 3. Since the clinker fragments are relatively large for the purpose of microscopy, they must be ground for XRD analysis. A ground specimen maximizes the number of particles in the analyzed volume, improves powder homogeneity and packing characteristics, reduces the propensity for preferred orientation, and minimizes microabsorption-related problems that may bias diffraction pattern intensities.

Specimens are crushed to sub-millimeter particles using a large mortar and pestle and then ground to produce a median particle size around 10 µm. Final grinding is accomplished using an orbital mill with agate cylinders as grinding elements. About 5 g of crushed clinker is ground using 15 mL of 200-proof ethanol for 6 min. The slurry is vacuum filtered using a 50 mm #2 filter and Buchner funnel by dispensing the initial grind slurry onto the filter followed by two rinse cycles using about 20 mL of ethanol and about 15 s of additional agitation in the mill to remove all solids. The ethanol typically dispenses clear on the second rinse, indicating all the sample has been deposited on the filter. The filter and

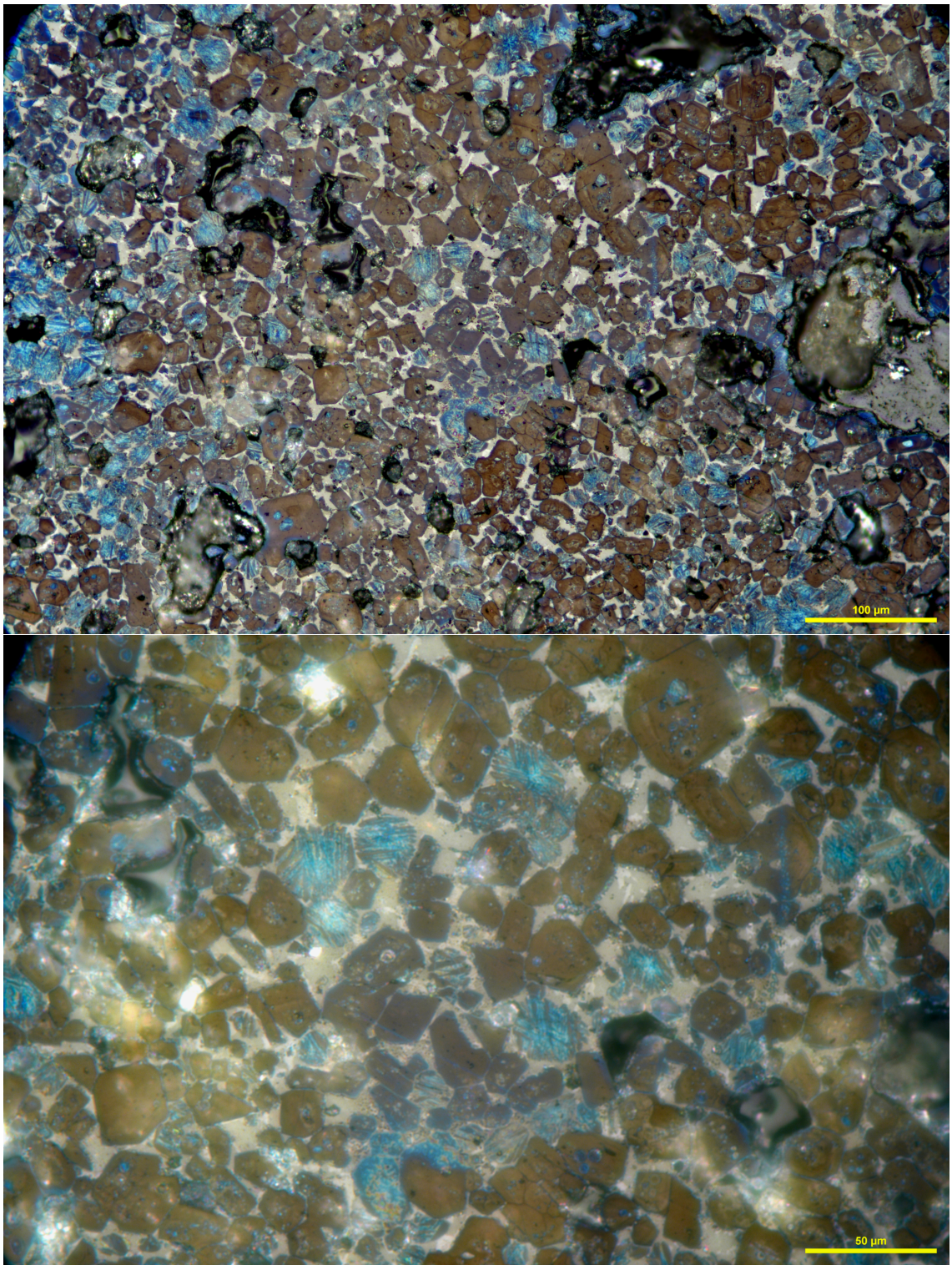

Fig. 2. Reflected light images of SRM2687a with low and high magnification after a 0.1 mol L^{-1} KOH etch followed by a 0.5 % nital etch to distinguish alite (brown), belite (blue), aluminate (gray), and ferrite (white), illustrating the fine-grained texture. Scale bars for upper (100 µm) and lower (50 µm) images are in yellow.

funnel is vacuum filtered to remove all liquid and then dried in an oven at 80 °C. Once the sample is dry, it is disaggregated and homogenized using an alumina mortar and pestle and the powder is placed in a glass vial for storage prior to processing.

Two selective extractions were employed to concentrate different phase groups and thereby facilitate phase identification: (1) potassium hydroxide - sucrose (KOHS) for the silicate phases and (2) salicyclic acid - methanol extractions for the interstitial phases. Concentrating the phase groups reduces pattern interference by reducing the total number of phases and increases detection limits by reducing the dilution of the specimen. The salicylic acid – methanol extraction provides an opportunity to make a second estimate of the interstitial phases which, when recalculated on a whole-clinker basis, are averaged with the bulk analyses to provide a test result. While the KOHS residue could be treated similarly, difficulties in consistent selective extractions preclude its use on a routine basis.

A test result is expressed as the mean of three replicate scans of the bulk clinker and three replicate scans of the salicylic acid-methanol extraction residue (Table 1). Samples were re-packed in the specimen holder for each replicate XRD scan. Scan data are collected from 11° to 77° 2-θ with a step size of 0.016° and 30 min collection time using Cu Kα radiation. Data below 18° was used for phase identification and not for refinement as beam overflow at lower angles may bias the diffraction peak intensities. Two different Rietveld codes were used to process the XRD data as they produced slightly different results for alite and belite; differences of approximately 2 % to 3 % for each. The powder diffraction patterns for these phases are highly overlapped and correlations between intensity, peak width and lattice parameters may have contributed to the difficulty in decomposing their respective diffraction patterns. To overcome this disagreement, each Rietveld code was treated as a distinct method and each was randomly assigned eleven samples to establish the data set along with the five SEM samples. Ideally, the test data across specimens (bulk and interstitial on a whole clinker basis) should agree as shown in Table 1 and any inconsistencies warrant further investigation. A more detailed description of the specimen preparation and analysis for powder diffraction is provided in [4]. The results of the XRD methods, labeled Code 1 and Code 2 [7] and the SEM/image analysis may be found in Appendix A.

3.3 Scanning Electron Microscopy

Five specimens of the as-received crushed clinker (about 4 mm fragments) were potted using a low viscosity resin, which was cured, cut and polished to 0.25 µm diamond paste. A set of $n = 7$ to $n = 9$ backscattered electron and X-ray images were collected by arbitrary selection of clinker fragments at one field per fragment. Examples of the clinker phase distribution and fine-grained texture are presented in Figure 4 at low and higher magnifications. In the upper image of Figure 4, the brightest phase occurs as clusters, or “nests”, of free lime. These nests represent residual CaO that did not react with SiO_2 in the kiln to form alite and are typically present in this clinker in low concentrations. The second brightest constituent is the ferrite phase which is easier seen in the lower image. In this clinker their are two types of ferrite textures: one with crystals a few micrometers and

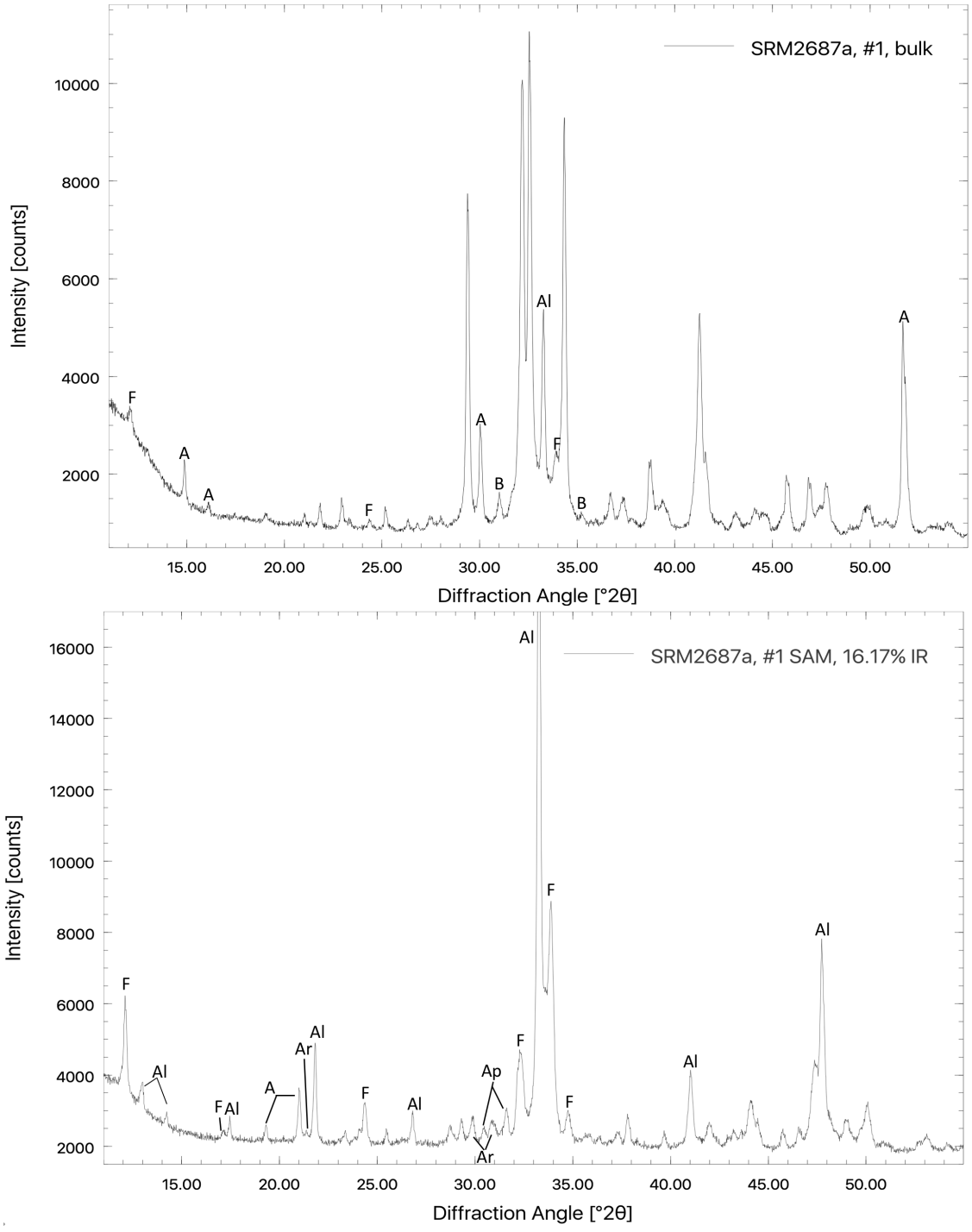

Fig. 3. X-Ray powder diffraction patterns for a whole-clinker (upper) and salicylic acid-methanol selective extraction of the interstitial phases (lower) with some of the unique diffraction peaks for each phase identified as alite (A), belite (B), aluminate (Al), ferrite (F), arcanite (Ar), and aphthitalite (Ap).

			Bulk Clinker			Whole Clinker Basis			SAM Residue Basis		
Phase	Mean	1s	1	2	3	1	2	3	1	2	3
Alite	58.0	0.1	57.9	58.0	58.1						
Belite	24.3	0.1	24.4	24.3	24.2						
Aluminate	9.0	0.1	9.0	9.1	8.9	9.1	9.1	9.1	56.2	56.1	56.2
Ferrite	6.4	0.3	6.7	6.7	6.8	6.2	6.2	6.2	38.3	38.3	38.1
Periclase	0.2	0.2	0.4	0.3	0.3	0.1	0.1	0.1	0.5	0.5	0.6
Arcanite	0.8	0.1	0.9	0.9	0.9	0.6	0.7	0.7	4.0	4.1	4.1
Aphthitalite	0.2	0.0	0.2	0.2	0.2	0.2	0.2	0.2	1.1	1.1	1.0
Free Lime	0.5	0.2	0.6	0.3	0.5	0.0	0.0	0.0	0.0	0.0	0.0

Table 1. Example of a single XRD test result expressed as a mean of the bulk and the SAM insoluble residue expressed on a whole-clinker basis for the interstitial phases. SAM extraction produced 16.2 % insoluble residue which is used to re-calculate the SAM residue basis values.

larger, and a second one that is a sub-micrometer network of ferrite within the aluminate matrix (Figure 5). While SEM will have difficulty distinguishing the fine-grained ferrite within the aluminate matrix, the XRD signal will not. In the light microscope, this interstitial phase texture may be described as undifferentiated. Complementing the backscattered electron signal and associated image is X-ray microanalysis, which may be used as a spot analysis qualitatively or quantitatively and to map element spatial distribution, where the signal intensity is roughly proportional to element concentration. X-ray imaging provides the chemical data in the form of an image that is registered (aligned) with the backscattered electron image and is useful for phase identification, visualization of element distribution, and to uniquely identify phases using combinations of images, as described in [4].

3.4 SEM Image Processing and Analysis

Quantitative analysis of the SEM image sets was performed using ImageJ[1,2] with a color segmentation plugin[3] that clusters pixels based upon pre-defined groups established by selecting regions typical for each phase. The first step involves processing the X-ray images to remove counts associated with the continuous background to reduce the adverse effects of this noise on the segmentation. An example of the energy-dispersive X-ray (EDS) spectrum from alite is provided in Figure 6 showing the characteristic element lines as peaks along with a continuous background. The first processing operation removes the signal associated with the characteristic background. The image brightness is increased to the point where the background signal becomes visible using the brightness and contrast settings of the image, and the intensity of the background is estimated by observing the pixel counts

[1]Certain trade names and company products are mentioned in the text to specify adequately the computer products and equipment needed to use this software. In no case does such identification imply endorsement by the National Institute of Standards and Technology of these computer products and equipment, nor does it imply that the products are necessarily the best available for the purpose.

[2]ImageJ: http://imagej.nih.gov/ij

[3]D. Sage, EPFL, Color Segmentation for ImageJ: http://bigwww.epfl.ch/sage/soft/colorsegmentation/

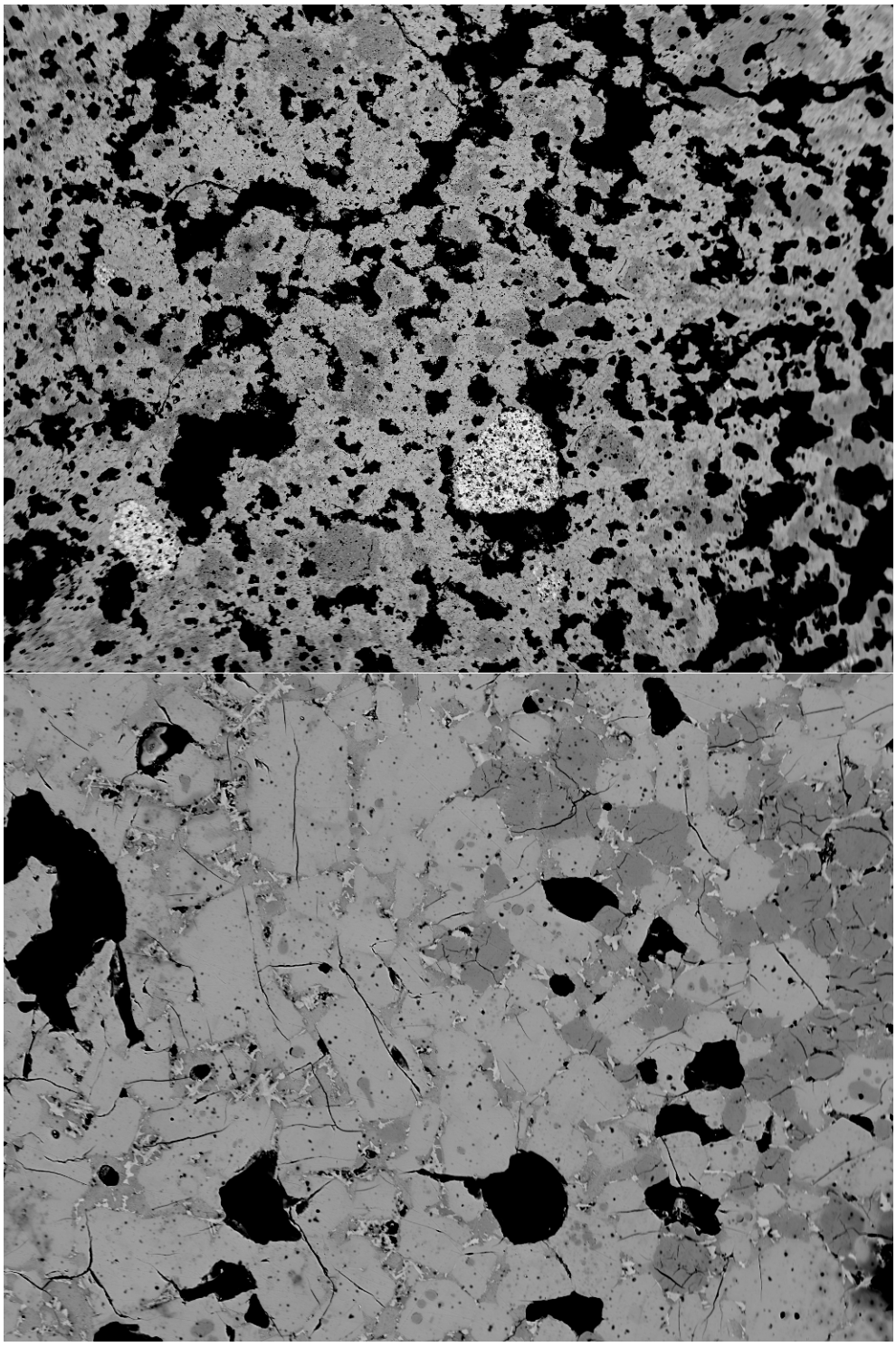

Fig. 4. SEM Backscattered electron images of SRM2687a showing nests of free lime (bright), abundant alite (intermediate gray), clusters of belite (darker gray), and pores (black) along with the fine-grained inter-mixed aluminate and ferrite comprising the matrix. Upper image field width is 1.2 mm, lower image field width is 300 µm, with both images captured at a 1024×768 pixel resolution.

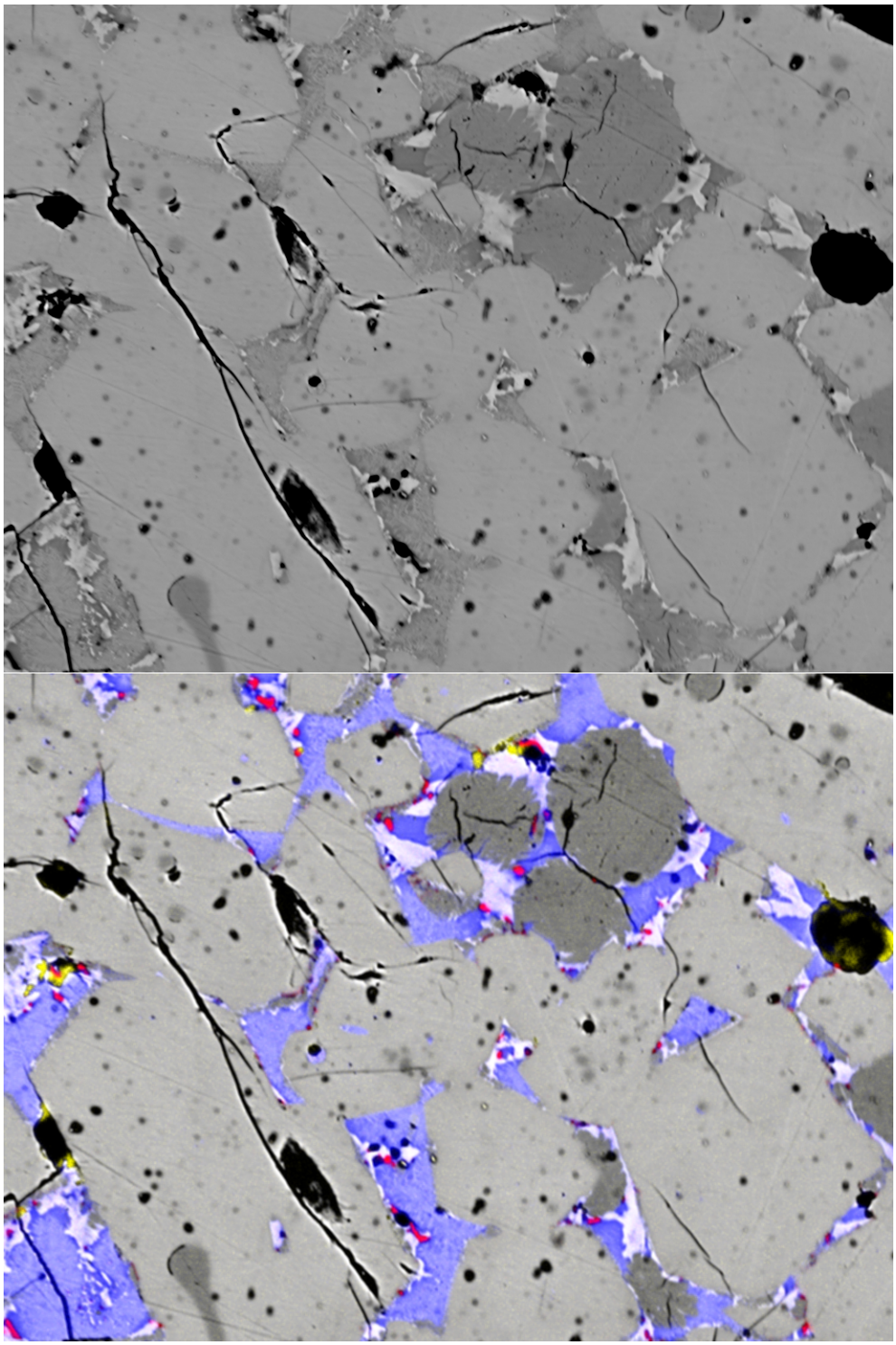

Fig. 5. SEM-backscattered electron image at higher magnification (field width is 150 µm) of the clinker matrix showing the fine-grained nature and inter-mixing of the aluminate and ferrite. Lower image is a composite SEM-BE and X-ray image set where Mg=red, Al=blue and S=yellow showing the locations and size of periclase (MgO, red) and alkali sulfates (K-$NaSO_3$, yellow).

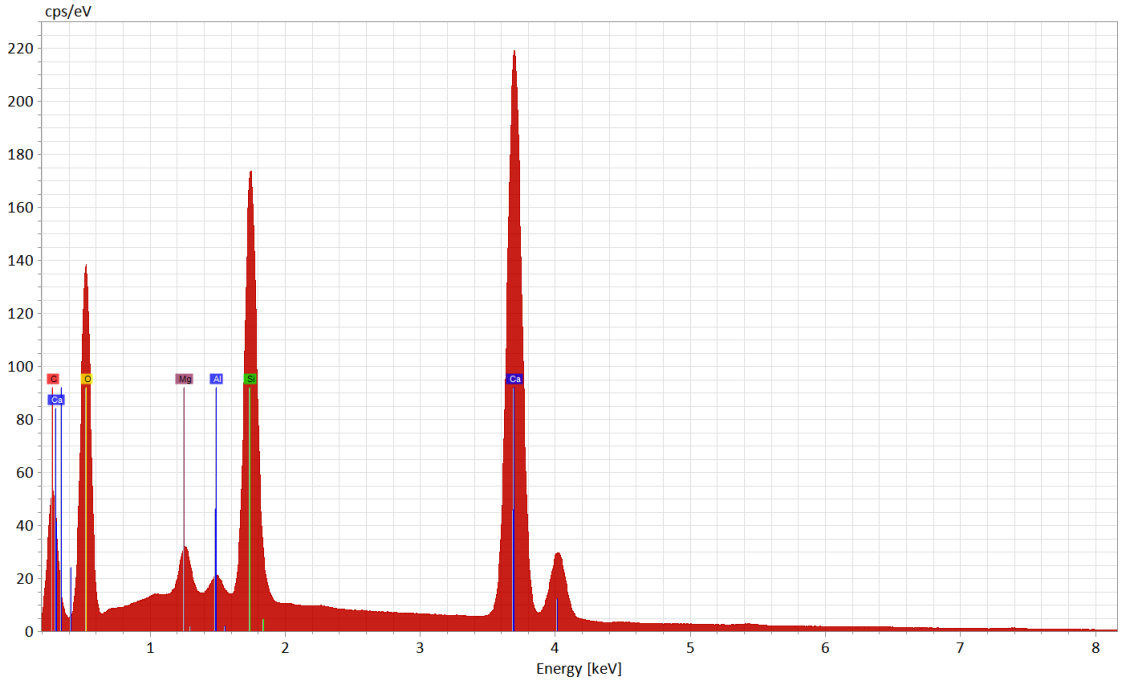

Fig. 6. Spectrum of alite shows the characteristic lines for calcium (Ca), silicon (Si), aluminum (Al), magnesium (Mg) and oxygen (O). The presence of carbon is from the thin film of carbon evaporated on the surface to dissipate excess charge.

in the ImageJ tool bar. Once the background intensity has been estimated, a subtraction operation is applied to all the pixels in the image. A de-noise or median operation follows to eliminate any lone pixels that remain. An example of these operations is shown with the sulfur image in Figure 7. Observation and estimating the background contribution to the images may also be facilitated through use of the gray level histogram. This segmentation operation was performed using the backscattered electron, aluminum, magnesium, and sulfur images (Figure 8) merged together to create a composite image expressed as a red-green-blue (RGB) image (Figure 9). This subset of images has been shown to be the minimum necessary to segment the constituent phases. Generally, most of the phases have unique image intensities in the backscattered electron image and those that do not (aluminate, periclase, alkali sulfates) are resolved and discriminated through addition of the X-ray images. The user can select a minimum set of images to merge into a RGB color image used to set the set of classes, or phases. For clinker, the addition of the aluminum image facilitates discrimination between aluminate and belite, which otherwise have essentially the same backscatter gray level. Segmentation of the alkali sulfate phases is accomplished with the addition of the sulfur, sodium, and potassium images. Regions typical for each phase (including the pores, which appear dark in all images) are selected to establish the phase classes and the classification algorithm groups all the pixels into the class in which they most likely belong (Figure 10). Given that the SEM/image analysis data are provided

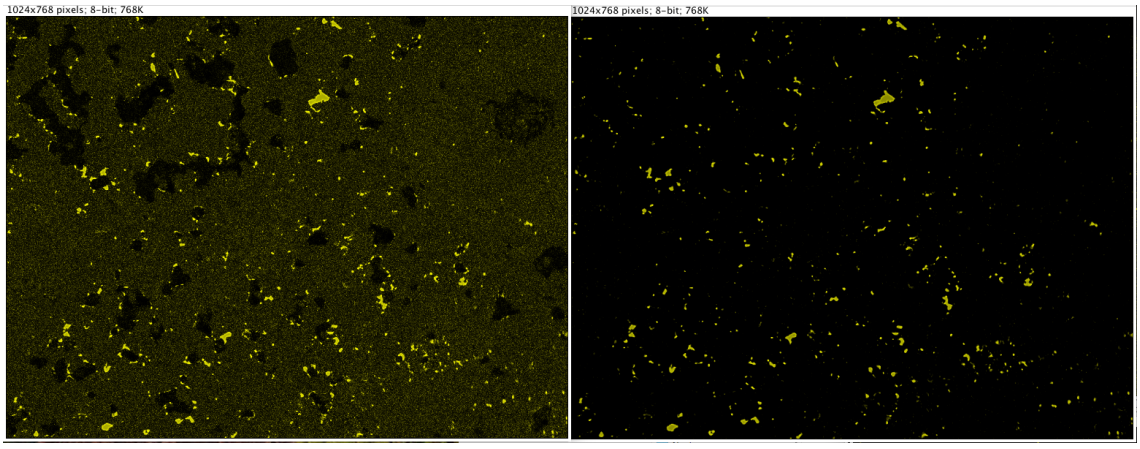

Fig. 7. Sulfur X-ray image before (left) and after (right) background subtraction and de-noising provides a cleaner image for the subsequent phase segmentation operation.

as area fractions, they must be recalculated on a mass basis to be consistent with the XRD data, using the phase densities provided in [8]. The data collection, processing and analysis are more completely described in [4].

4. Consensus Means and Uncertainties

There are a variety of methods for estimating consensus means and the associated uncertainties [13]. The grand mean is simply the average of all the data from all methods. This does not take into account either within method variability or between method variability. The mean of means is an early consensus method as an unweighted mean of method means. While this approach takes between method variability into account, it does not include within method variability. The Graybill-Deal method is a weighted mean where the weights are determined by the within method variability. However, this method does not take between method variability into account.

The DerSimonian-Laird (DSL) [10] and the Vangel-Rukhin (VR) [14] approaches take both the within method variance and the between method variance into account. The Vangel-Rukhin method is essentially the maximum likelihood (ML) approach. Although ML approach has excellent statistical properties, these properties are asymptotic and we have relatively few methods. The DSL approach starts with the Graybill-Deal estimate, but then adds a correction to account for the between method variability. The DSL approach can be used for either a small number of methods or a large number of methods. Our primary reason for choosing DSL over Vangel-Rukhin is that we have a small number of methods.

The DSL uncertainties were determined using the Horn-Horn-Duncan (HHD) method for the variance of weighted means. The generic HHD method is described in [11] and the application of HHD to DSL estimates is given in [15] (specifically, see equation 19 on page 327). In addition, uncertainties are computed using a parametric bootstrap [12] method.

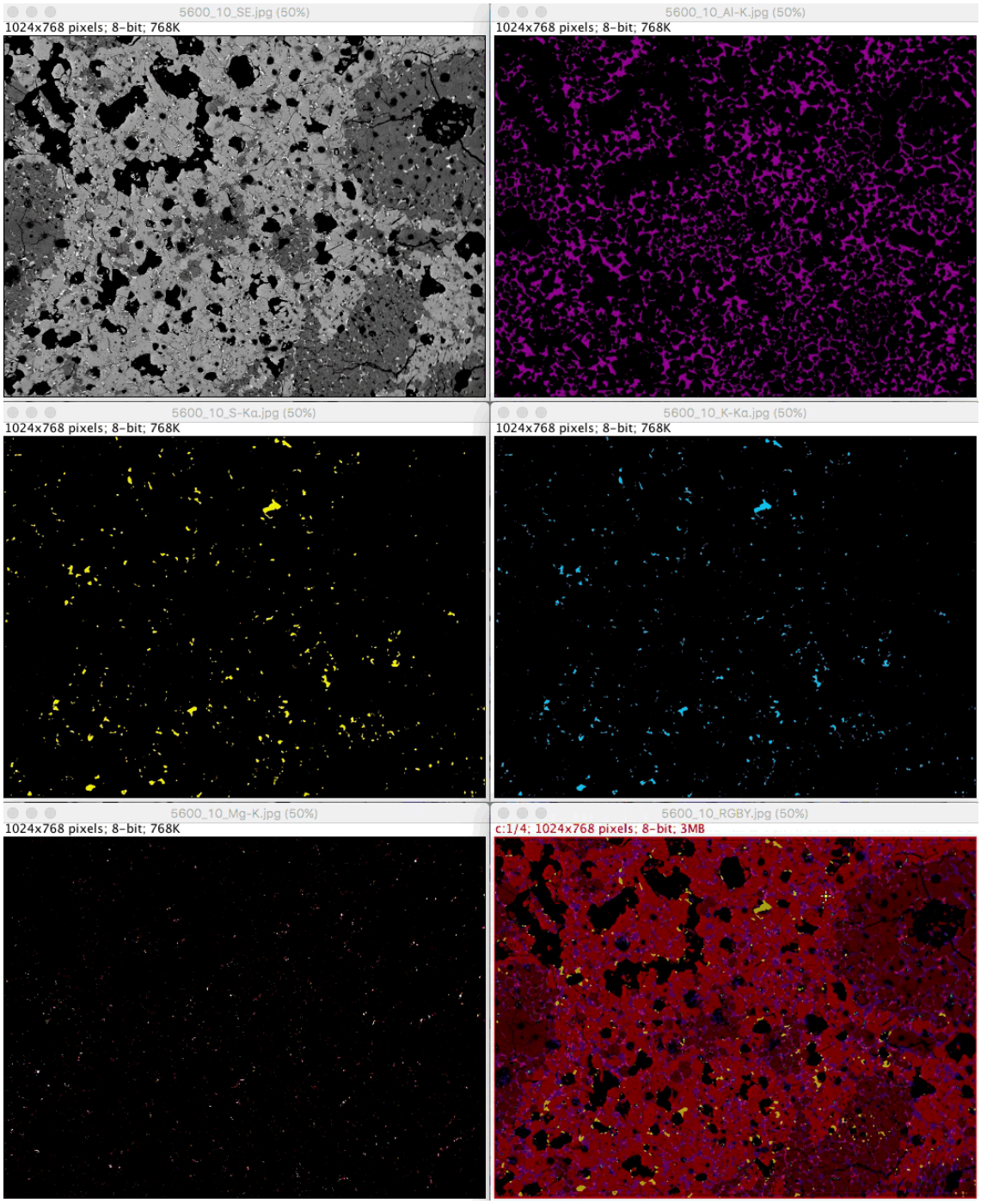

Fig. 8. SEM Image set for backscattered electron, aluminum, potassium, sulfur, magnesium and a color-composite image where these images have been merged to create a false-color image ready for phase identification and segmentation

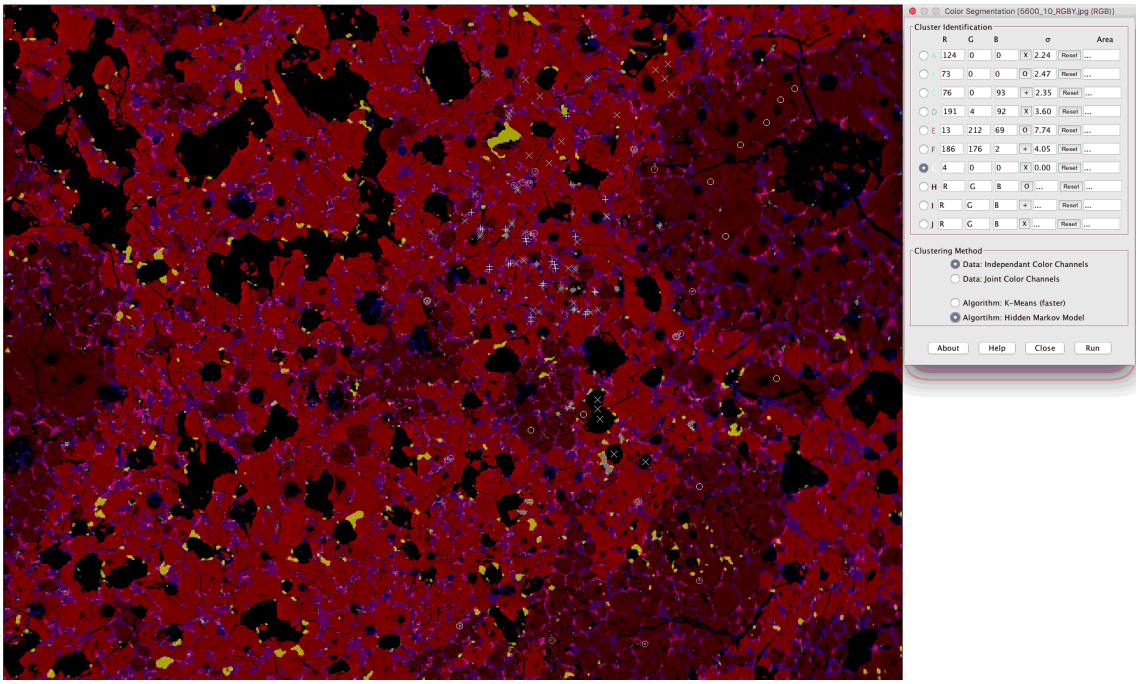

Fig. 9. RGB Image from Figure 6 with typical regions marked for each phase, which includes porosity.

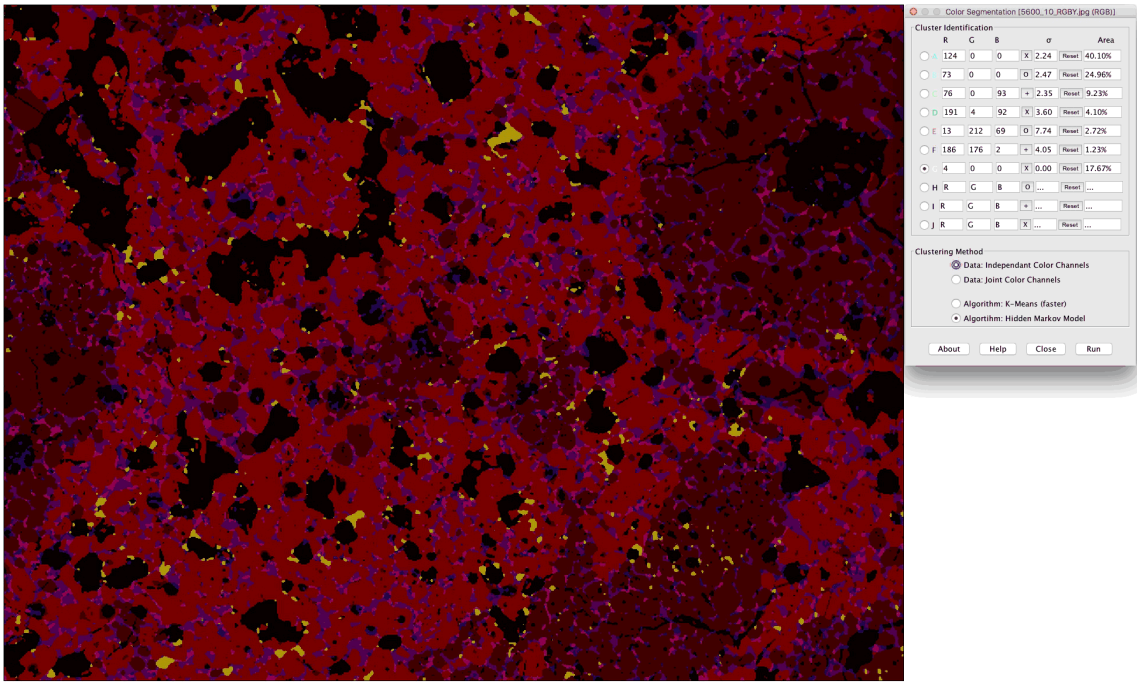

Fig. 10. Segmented image (lower) with calculated area fractions for each cluster mirrors the composite image shown in Figure 9, indicating a successful segmentation. From the top, the cluster identifications are alite, belite, aluminate, ferrite, periclase, alkali sulfate, and porosity.

See [16] for a description of the parametric bootstrap model used here. The bootstrap is a resampling method that can be used to obtain uncertainty estimates when analytic methods are unavailable or the underlying assumptions for the analytic method are not satisfied. In the context of the consensus means analysis used here, the bootstrap is used as a check. That is, if the bootstrap uncertainties are significantly larger than the HHD uncertainties, this is an indication that the underlying normality assumptions of the DSL method are not satisfied.

For measurements where multiple methods were used, the values and uncertainties (certified or reference) are calculated by combining the results from all of the measurement methods using the following model:

$$y_{ij} = \mu + m_i + \varepsilon_{ij};\ i = 1,2,...,n_{mm};\ j = 1,2,...n_i \tag{1}$$

where i indexes measurement methods, j indexes replication within a measurement method, n_{mm} represents the number of measurement methods, n_i represents the number of replications within a measurement method, $m_i \overset{iid}{\sim} N(0,\sigma_m^2)$, and $\varepsilon_{ij} \overset{iid}{\sim} N(0,\sigma_i^2)$ independently of m_i. The values (certified or reference) are estimates of μ, say $\hat{\mu}$, in (1), and the estimator employed is the DerSimonian-Laird (DSL). The uncertainties were determined using the HHD method for variances described in [11] and also with the bootstrap method [12]. Results are presented for both methods. The values, standard uncertainties, and expanded uncertainties for the Horn-Horn-Duncan method are listed in Table 2. The values, standard uncertainties, coverage factors, and expanded uncertainties for the bootstrap method are listed in Table 3.

Plots for each phase are presented in Figures 11 through 14, with code 1 and 2 being the two different XRD processing codes. The consensus means and associated uncertainties for the various consensus methods described in [13] are plotted in the left-hand portion while the data for XRD method 1 (Code 1) and XRD method 2 (Code 2) and SEM analyses are shown in the right-hand portion of each plot. The HHD variances were slightly more conservative than the bootstrap variances and are the recommended values. The DSL estimates were also consistent with the Vangel-Rukhin maximum likelihood estimates. Certified values for alite, belite, aluminate, and ferrite are based upon the two test methods while reference values for periclase, arcanite, aphthitalite, and free lime are provided based upon the X-ray powder diffraction results.

Table 2 provides the results for the multiple method data. These results were obtained using the DerSimonian-Laird estimate for the consensus mean. The standard uncertainties are based on the Horn-Horn-Duncan variance estimate.

4.1 Bulk Chemistry Reference Values

Reference values represent best estimates of the true value where all known or suspected sources of bias have not been fully investigated [9]. The bulk chemical composition for this clinker was measured by a single method, X-ray fluorescence analysis, by an outside collaborating laboratory. The bulk chemical data are expressed as oxides as is the convention

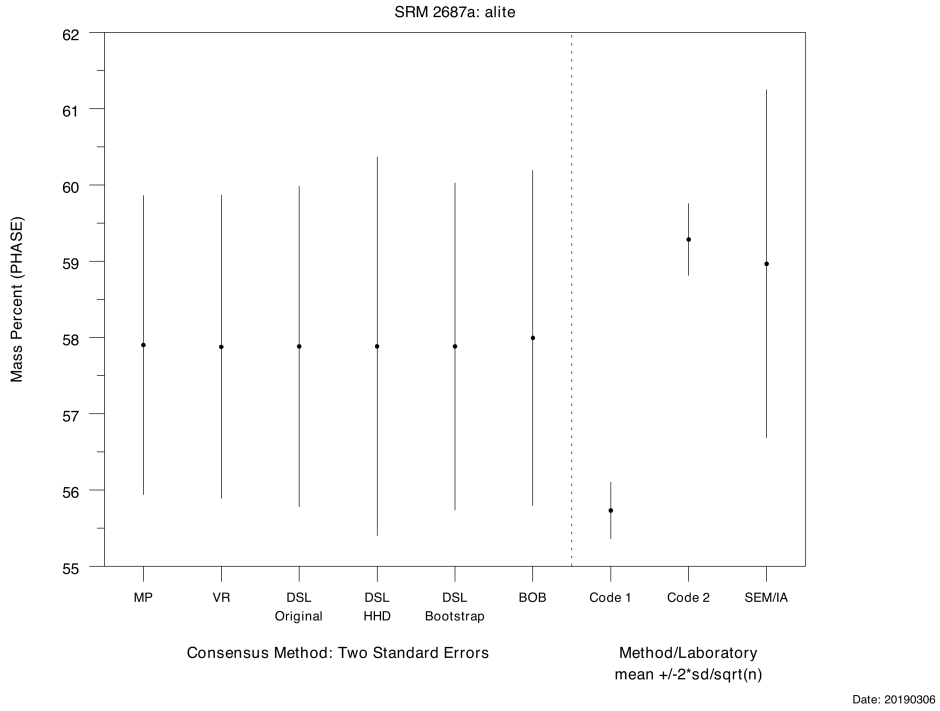

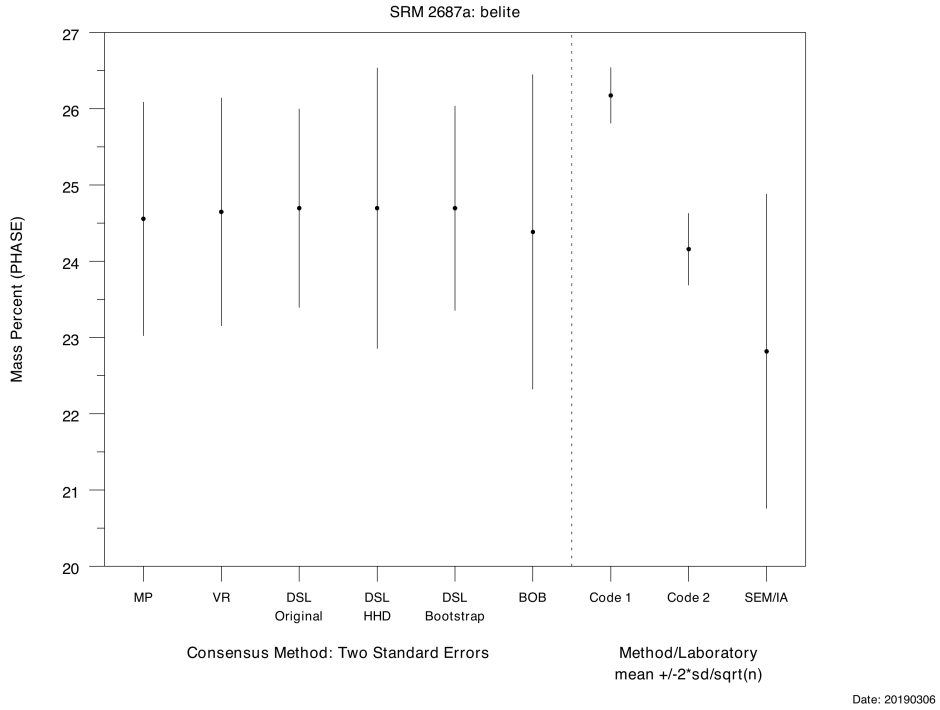

Fig. 11. Consensus means expressed as mass percent by method for alite (upper) and belite (lower).

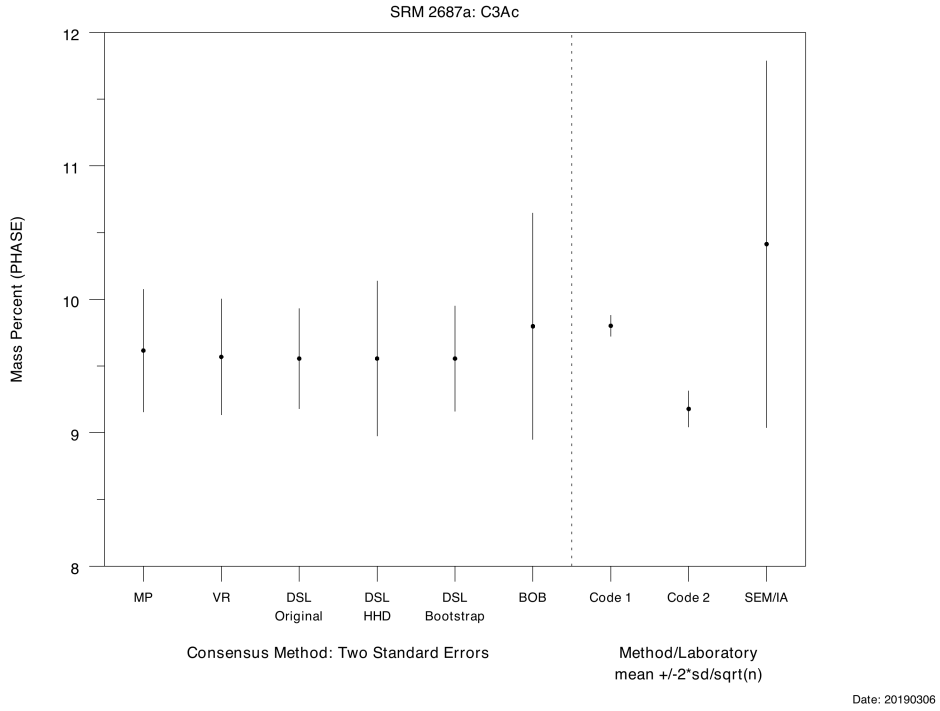

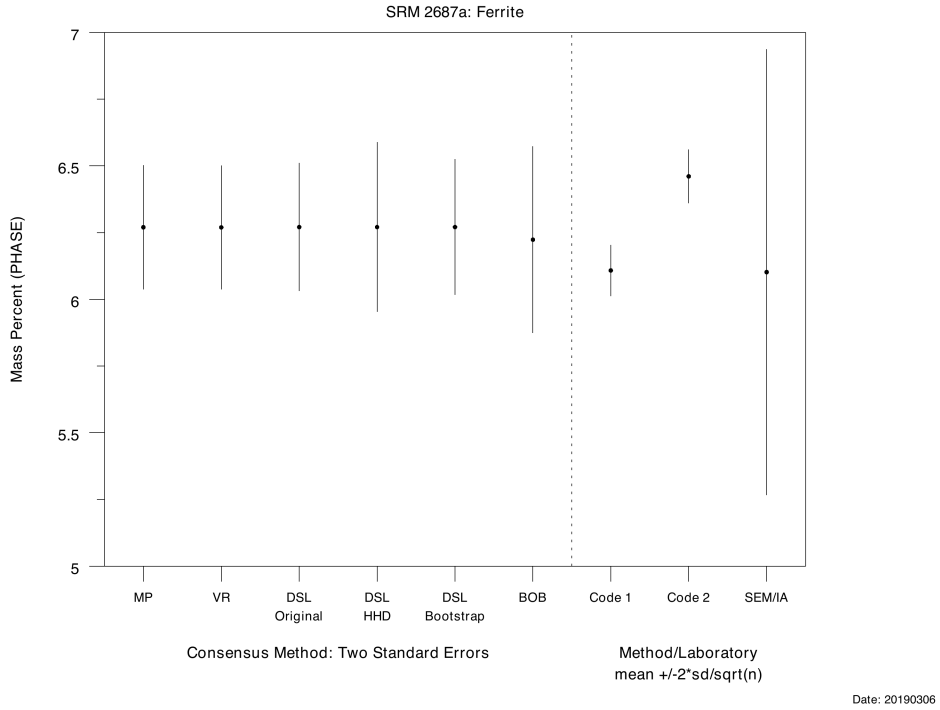

Fig. 12. Consensus means expressed as mass percent by method for aluminate (upper) and ferrite (lower).

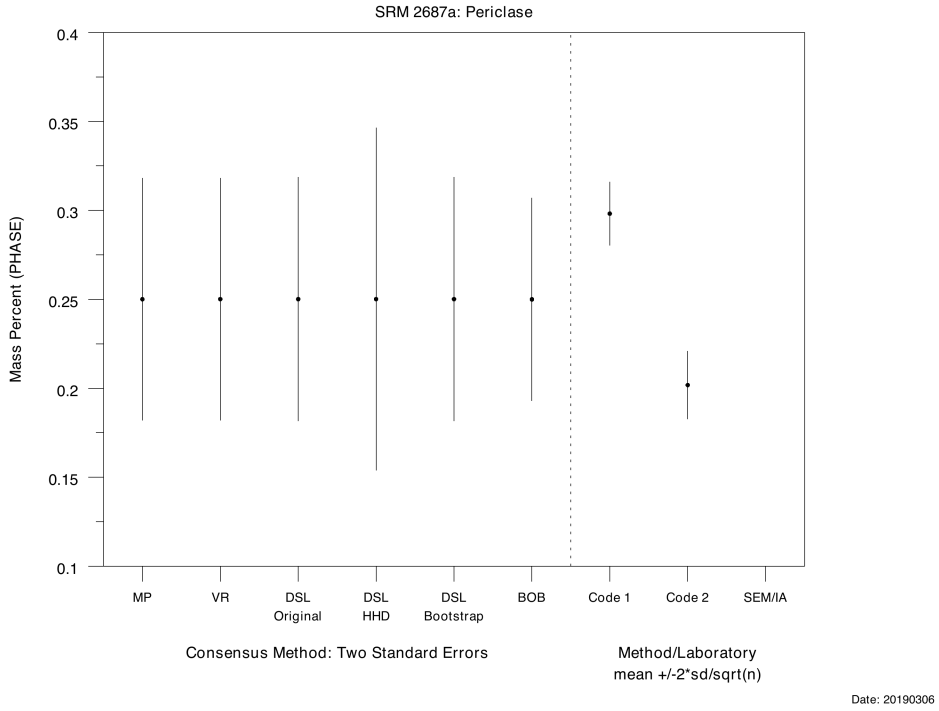

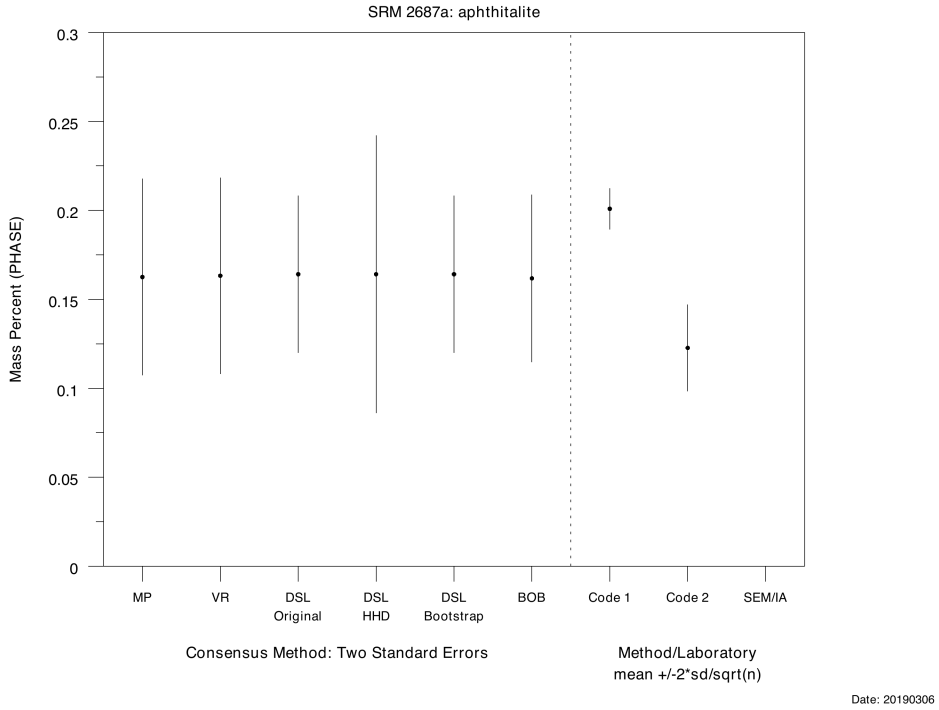

Fig. 13. Consensus means expressed as mass percent by method for periclase (upper) and aphthitalite (lower).

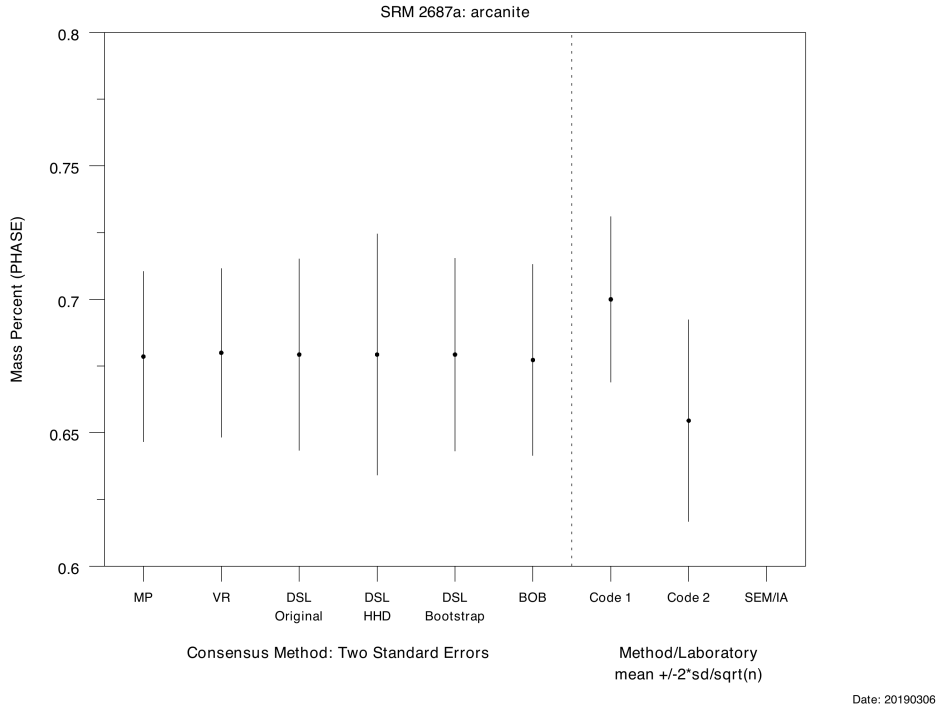

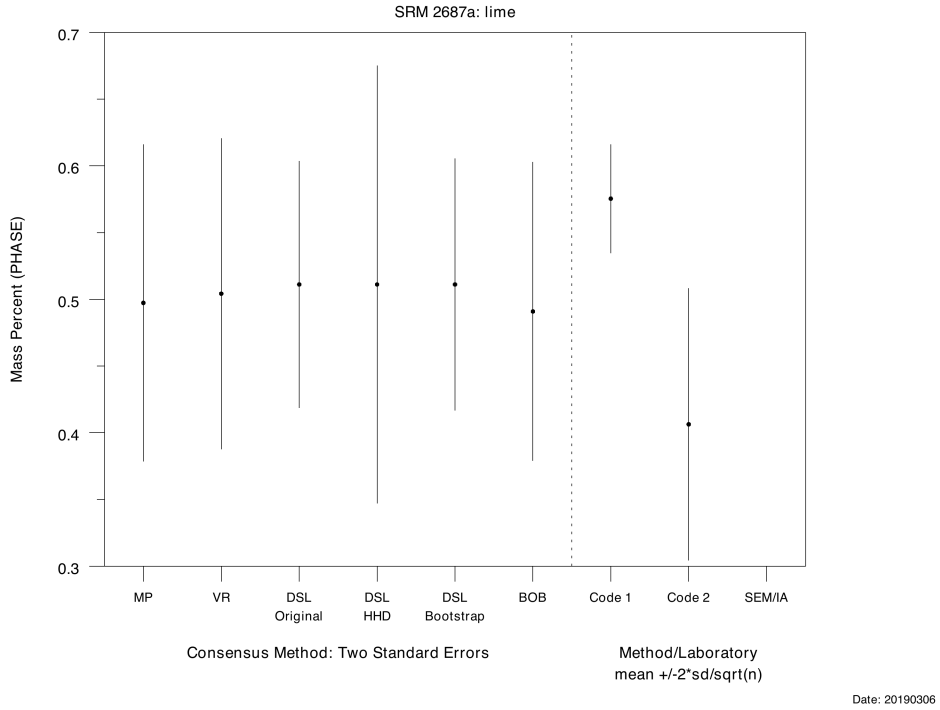

Fig. 14. Consensus means expressed as mass percent by method for arcanite (upper) and lime (lower).

Table 2. Consensus Means Based Upon DerSimonian-Laird Horn-Horn-Duncan Results for Multiple Method Data

Constituent	Consensus Mean	Standard Uncertainty	k=2 Expanded Uncertainty	Coverage Factor	95 % Lower Confidence Limit	95 % Upper Confidence Limit
Alite	57.883	1.243	2.486	4.303	52.535	63.231
Belite	24.696	0.921	1.843	4.303	20.731	28.661
Aluminate	9.556	0.291	0.582	4.303	8.305	10.808
Ferrite	6.271	0.159	0.318	4.303	5.586	6.956
Periclase	0.250	0.058	0.096	12.706	−0.362	0.862
Arcanite	0.679	0.023	0.045	12.706	0.392	0.967
Aphthitalite	0.164	0.039	0.078	12.706	−0.332	0.660
Free Lime	0.511	0.082	0.164	12.706	−0.532	1.554

Table 3. Standard Uncertainties Based Upon DerSimonian-Laird Bootstrap Results for Multiple Method Data

Constituent	Consensus Mean	Bootstrap Uncertainty	Coverage Factor	Bootstrap Expanded Uncertainty
Alite	57.883	1.073	1.961	2.105
Belite	24.696	0.671	1.977	1.327
Aluminate	9.556	0.198	1.970	0.390
Ferrite	6.271	0.127	1.969	0.251
Periclase	0.250	0.034	1.972	0.068
Arcanite	0.679	0.018	1.968	0.036
Aphthitalite	0.164	0.022	1.966	0.043
Free Lime	0.511	0.047	1.977	0.093

in the cement industry, and these specimens would be useful for purposes of expanding calibration curves for specific analytes. A set of five samples was distributed, with each sample split into three individual specimens for analysis. The test results (Table 4) represent the overall mean of the five individual specimens tested in triplicate. The laboratory providing these data noted that the sulfur determination was based on a cement curve which, because of the calcium sulfate addition, would typically have a greater mass of sulfur. Given the sulfur determination uses an extrapolated calibration curve, it may be biased and therefore should be used with caution.

Table 4. Reference Values for Bulk Chemistry by X-Ray Fluorescence Analysis

Oxide[a]	SiO_2	Al_2O_3	Fe_2O_3	CaO	MgO
Grand Mean	22.072	5.470	2.403	66.172	1.035
St. Dev.	0.073	0.043	0.135	0.334	0.007
Oxide	SO_3	Na_2O	K_2O	TiO_2	P_2O_5
Grand Mean	0.695	0.103	0.702	0.246	0.524
St. Dev.	0.033	0.003	0.017	0.001	0.008
Oxide	Mn_2O_3	SrO	ZnO	Clinker LOI	Total
Grand Mean	0.031	0.090	0.028	0.49	100.058
St. Dev.	0.002	0.001	0.002	0.21	0.181

[a] Reference values are means expressed as oxide means from five individual clinker specimens each with triplicate specimens.

Acknowledgments

Support from the Standard Reference Materials Program for the development of this SRM is acknowledged. Assistance in LaTeX formatting by Jeff Bullard and Kathryn Miller is greatly appreciated as are the comments and suggestions of reviewers.

References

[1] ASTM C 150 (2017) Standard specification for portland cement. (ASTM International, West Conshohocken, PA).

[2] Stutzman P, Heckert A, Tebbe A, Leigh S (2014) Uncertainty in Bogue-calculated phase composition of hydraulic cements, *Cement and Concrete Research* 61–62:40–48. https://doi.org/10.1016/j.cemconres.2014.03.007

[3] ASTM C 1356 (2017) Standard test method for determination of the proportion of phases in portland cement and portland-cement clinker using X-ray powder diffraction analysis. (ASTM International, West Conshohocken, PA).

[4] Stutzman P, Feng P, Bullard J (2016) Phase analysis of portland cement by combined X-ray powder diffraction and scanning electron microscopy, *Journal of Research of the National Institute of Standards and Technology* 121:47–107. https://doi.org/10.6028/jres.121.004

[5] Campbell DH (1999) *Microscopical Examination and Interpretation of Portland Cement and Clinker* (Portland Cement Association, Skokie, IL).

[6] Hofmanner F (1975) *Microstructure of Portland Cement Clinker* (Rheintaler Druckerei und Verlag AG, Heerbrugg, Switzerland).

[7] Dobelin N, Kleeberg, R (2015) Profex: a graphical user interface for the Rietveld refinement program BGMN, *Journal of Applied Crystallography* 48:1573–1580. doi:10.1107/S1600576715014685

[8] Taylor HFW (1997) *Cement Chemistry* (Thomas Telford, London)

[9] May W, Parris R, Beck C, Fassett J, Greenberg R, Guenther F, Kramer G, Wise S, Gills T, Colbert J, Gettings R, McDonald B (2000) Definitions of terms and modes used at NIST for value-assignment of reference materials for chemical measurements. NIST SP 260 (NIST, Gaithersburg, MD).

[10] DerSimonian R, Laird N (1986) Meta-analysis in clinical trials, *Controlled Clinical Trials* 7:177–188.

[11] Horn RA, Horn SA, Duncan DB (1975) Estimating heteroscedastic variance in linear models, *Journal of the American Statistical Association* 70:380–385.

[12] Efron B, Tibshirani RJ (1993) *An Introduction to the Bootstrap* (Chapman and Hall/CRC Monographs on Statistics and Applied Probability).

[13] Heckert A, Filliben J (2016) https://www.itl.nist.gov/div898/software/dataplot /refman1/auxillar/consmean.htm

[14] Vangel M and Rukhin A (1999) Maximum Likelyhood Analysis for Heteroscedastic One-Way Random Effects ANOVA in Interlaboratory Studies *Biometrics* Vol. 55, pp. 129-136.

[15] Rukhin A, Weighted Means Statistics in Interlaboratory Studies, *Metrologia* Vol. 46, pp. 323-331

[16] Possolo A (2015) Simple Guide for Evaluating and Expressing the Uncertainty of NIST Measurement Results *NIST Technical Note 1900* Department of Commerce, pp. 48-49

Appendix A: Supplemental Materials

1 Test Results for XRD and SEM Analyses

Table 5. XRD (1, 2) and SEM/IA (3) Data Summary

Sample	Method	Alite	Belite	C_3Ac	Ferrite	Periclase	Arcanite	Aphthitalite	Lime	SEM/IA Method
1	1	56.16	25.43	9.56	6.61	0.44	0.90	0.30	0.61	1
200	1	58.00	24.44	9.37	5.93	0.24	0.82	0.23	0.66	1
200	1	57.01	24.94	9.77	6.10	0.29	0.78	0.20	0.50	1
800	1	55.65	26.36	9.93	5.80	0.28	0.67	0.23	0.58	1
800	1	55.74	26.37	9.89	5.89	0.24	0.78	0.22	0.48	1
1000	1	56.34	25.64	9.63	6.12	0.30	0.64	0.19	0.59	1
1200	1	56.22	26.20	9.18	6.50	0.27	0.78	0.19	0.47	1
1400	1	55.77	26.10	9.89	5.95	0.27	0.73	0.21	0.63	1
2000	1	55.58	26.54	9.82	6.11	0.25	0.73	0.20	0.60	1
2200	1	55.84	26.08	9.72	6.17	0.35	0.71	0.23	0.67	1
2600	1	55.42	26.44	9.82	6.22	0.29	0.72	0.18	0.60	1
2800	1	55.88	25.98	9.98	5.93	0.32	0.66	0.20	0.62	not used
3000	1	56.22	25.37	9.98	6.33	0.21	0.65	0.20	0.62	
3400	1	54.95	27.21	9.66	5.99	0.34	0.72	0.21	0.67	
3800	1	56.38	25.39	9.57	6.11	0.34	0.74	0.19	0.57	
4000	1	55.29	26.32	9.90	6.28	0.30	0.66	0.20	0.54	
5800	1	55.29	26.32	9.81	6.28	0.30	0.69	0.18	0.54	
6000	1	55.09	26.65	9.77	6.37	0.34	0.70	0.18	0.63	
6400	1	55.75	26.53	9.87	5.80	0.29	0.74	0.19	0.64	
7400	1	55.99	25.97	9.71	6.18	0.28	0.66	0.21	0.55	
8000	1	56.63	24.96	9.88	6.32	0.29	0.74	0.21	0.63	
8200	1	54.81	26.96	9.96	6.40	0.31	0.64	0.16	0.49	
8400	1	55.84	25.99	9.61	6.13	0.34	0.71	0.23	0.66	
1	2	59.78	23.17	8.70	6.59	0.18	0.75	0.15	0.32	
200	2	60.46	24.94	9.77	6.10	0.29	0.78	0.20	0.50	
200	2	60.93	22.36	9.06	6.24	0.17	0.80	0.15	0.60	
800	2	58.54	24.36	9.14	6.37	0.20	0.57	0.17	0.60	
800	2	58.74	24.52	8.96	6.53	0.19	0.73	0.11	0.38	
1000	2	59.58	23.79	8.94	6.46	0.19	0.59	0.11	0.40	
1200	2	58.39	24.99	9.04	6.60	0.20	0.76	0.11	0.00	
1400	2	59.51	23.45	9.16	6.48	0.18	0.63	0.11	0.53	
2000	2	58.42	24.88	8.98	6.67	0.20	0.64	0.13	0.41	
2200	2	59.35	23.86	9.12	6.49	0.19	0.63	0.15	0.58	
2600	2	58.98	24.28	9.33	6.47	0.21	0.52	0.12	0.42	
2800	2	58.81	24.18	9.32	6.31	0.19	0.60	0.15	0.55	not used
3000	2	59.43	23.70	9.33	6.55	0.16	0.61	0.10	0.33	2
3400	2	58.45	25.00	9.01	6.37	0.17	0.64	0.14	0.55	2
3800	2	60.05	23.38	8.95	6.26	0.19	0.67	0.13	0.39	2
4000	2	58.75	24.34	9.18	6.55	0.21	0.55	0.13	0.47	2
5800	2	58.98	24.51	9.11	6.48	0.21	0.62	0.05	0.26	2
6000	2	58.68	24.62	9.22	6.51	0.19	0.63	0.11	0.47	2
6400	2	59.26	24.09	9.05	6.42	0.19	0.63	0.11	0.52	2
7400	2	59.35	23.80	8.81	6.47	0.16	0.61	0.15	0.44	2
8000	2	60.58	22.42	9.26	6.62	0.20	0.66	0.09	0.41	2
8200	2	58.04	25.25	9.32	6.68	0.19	0.53	0.06	0.30	2
8400	2	59.30	24.09	8.96	6.39	0.21	0.67	0.10	0.46	2
5600	3	56.93	21.28	13.06	7.30					SEM/IA
5000	3	56.27	26.10	9.72	6.33					SEM/IA
4800	3	60.55	22.67	9.78	5.46					SEM/IA
4600	3	58.64	23.87	10.35	4.91					SEM/IA

2. Bulk Chemistry by X-Ray Fluorescence Analysis based upon five samples run in triplicate

Table 6. Mean bulk oxide values for five clinker specimens for n=3 individual replicates.

	Sample 1		Sample 2		Sample 3	
Component	$\bar{x}$[a]	s	$\bar{x}$	s	$\bar{x}$	s
SiO_2	21.986	0.047	22.159	0.047	22.087	0.088
Al_2O_3	5.395	0.031	5.495	0.032	5.497	0.035
Fe_2O_3	2.624	0.003	2.441	0.003	2.319	0.011
CaO	65.654	0.071	66.207	0.200	66.075	0.178
MgO	1.044	0.004	1.025	0.005	1.033	0.002
SO_3	0.750	0.002	0.680	0.008	0.682	0.007
Na_2O	0.102	0.007	0.105	0.008	0.103	0.005
K_2O	0.695	0.002	0.685	0.003	0.695	0.002
TiO_2	0.245	0.003	0.246	0.002	0.248	0.002
P_2O_5	0.522	0.001	0.520	0.001	0.517	0.003
Mn_2O_3	0.033	0.001	0.031	0.003	0.030	0.003
SrO	0.089	0.001	0.089	0.001	0.089	0.002
ZnO	0.029	0.001	0.030	0.001	0.030	0.000
LOI	0.85		0.43		0.35	
Total	100.021		100.145		99.758	

	Sample 4		Sample 5		Grand	
	$\bar{x}$	s	$\bar{x}$	s	$\bar{\bar{x}}$	s
SiO_2	22.009	0.081	22.121	0.081	22.072	0.073
Al_2O_3	5.486	0.055	5.478	0.055	5.470	0.043
Fe_2O_3	2.322	0.014	2.309	0.014	2.403	0.135
CaO	66.452	0.194	66.471	0.194	66.172	0.334
MgO	1.040	0.011	1.035	0.011	1.035	0.007
SO_3	0.666	0.026	0.696	0.026	0.695	0.033
Na_2O	0.098	0.006	0.105	0.006	0.103	0.003
K_2O	0.706	0.040	0.729	0.040	0.702	0.017
TiO_2	0.247	0.002	0.246	0.002	0.246	0.001
P_2O_5	0.524	0.021	0.537	0.021	0.524	0.008
Mn_2O_3	0.029	0.003	0.032	0.003	0.031	0.002
SrO	0.091	0.001	0.091	0.001	0.090	0.001
ZnO	0.026	0.001	0.027	0.001	0.028	0.002
LOI	0.46		0.36		0.49	0.21
Total	100.158		100.208		100.058	0.181

[a] Five individual clinker samples where each mean result is the average of three separate specimen preparations.